



## *In vitro* labelling of muscle type nicotinic receptors using a fluorophore-conjugated pinnatoxin F derivative



Shane D. Hellyer<sup>a</sup>, Andrew I. Selwood<sup>b</sup>, Roel van Ginkel<sup>b</sup>, Rex Munday<sup>c</sup>,  
Phil Sheard<sup>d</sup>, Christopher O. Miles<sup>e,f</sup>, Lesley Rhodes<sup>b</sup>, D. Steven Kerr<sup>a,\*</sup>

<sup>a</sup> Department of Pharmacology and Toxicology, University of Otago School of Medical Sciences, Dunedin, New Zealand

<sup>b</sup> Cawthron Institute, 98 Halifax Street East, Private Bag 2, Nelson, New Zealand

<sup>c</sup> AgResearch, Private Bag 3123, Hamilton, New Zealand

<sup>d</sup> Department of Physiology, University of Otago School of Medical Sciences, Dunedin, New Zealand

<sup>e</sup> National Veterinary Institute, PB 750 Sentrum, 0106 Oslo, Norway

<sup>f</sup> Department of Pharmaceutical Chemistry, School of Pharmacy, University of Oslo, P.O. Box 1068 Blindern, N-0316 Oslo, Norway

### ARTICLE INFO

#### Article history:

Received 5 February 2014

Received in revised form 2 May 2014

Accepted 7 May 2014

Available online 2 June 2014

#### Keywords:

Fluorescent pinnatoxin

Confocal imaging

NMJ

Endplate

Nicotinic receptors

### ABSTRACT

Fluorescent molecules are regularly utilised to study ligand–receptor interactions. Many ligands for nicotinic receptors have been conjugated with fluorophores to study receptor kinetics, recycling and ligand binding characteristics. These include small agonist molecules, as well as large peptidic antagonists. However, no small molecule antagonists have been investigated using this method. Pinnatoxin F is a newly discovered non-peptidic muscle type nicotinic receptor antagonist produced by the marine dinoflagellate species *Vulcanodinium rugosum*. This molecule has the potential for conjugation to a fluorophore, allowing subsequent visualisation of interactions with nicotinic receptors. Pinnatoxin F was modified by addition of diaminopolyether spacers, to which a fluorophore (VivoTag<sup>®</sup> 645) was conjugated. The fluorescent pinnatoxin was then applied to muscle sections from *thy1-YFP-H* transgenic mice, which express YFP in motor nerves, to allow direct visualization of fluorescent binding at the neuromuscular junction. The addition of both the diaminopolyether spacer and the VivoTag<sup>®</sup> 645 reduced the potency of pinnatoxin F, as evidenced by a reduction in *in vitro* neuromuscular blocking activity and *in vivo* toxicity. Despite this reduced potency, the fluorescent molecule selectively labelled endplate regions in *thy1-YFP* mouse muscle sections and this labelling was inhibited by pre-exposure of muscle sections to native pinnatoxin F or the nicotinic antagonist  $\alpha$ -bungarotoxin. This study proves nicotinic receptor binding activity of pinnatoxin F and is the first example of a fluorophore-conjugated small-molecule antagonist for nicotinic receptors. These results indicate the potential for other small-molecule nicotinic receptor antagonists to be fluorescently labelled and used as probes for specific nicotinic receptor subtypes.

© 2014 Elsevier Ltd. All rights reserved.

### 1. Introduction

Ligand binding and receptor function can be studied using fluorescent ligands, facilitating direct visualization of binding sites and molecular re-organisation during receptor-gating. Nicotinic receptors (nAChRs) are pentameric ligand-gated ion channels that mediate signal

\* Corresponding author. Department of Pharmacology and Toxicology, University of Otago, Dunedin, Otago 9001, New Zealand. Tel.: +64 3 479 9142.

E-mail addresses: [steve.kerr@stonebow.otago.ac.nz](mailto:steve.kerr@stonebow.otago.ac.nz), [steve.kerr@otago.ac.nz](mailto:steve.kerr@otago.ac.nz) (D.S. Kerr).

transduction at the neuromuscular junction (NMJ) and have been probed using fluorescent ligands for some 40 years. Fluorescent agonists are most commonly used to drive receptors into a desensitized state that can be more easily probed (Auerbach, 2003; Edelstein et al., 1997). Initial attempts involved the creation of fluorescent ACh analogues, through the attachment of fluorophores such as dansyl, pyrene, *N*-(7-nitrobenz-2-oxa-1,3-diazol-4-yl) (NBD) and 7-diethylaminocoumarin (DEAC) (Barrantes et al., 1975; Cohen and Changeux, 1973; Jürss et al., 1979; Krieger et al., 2008; Song et al., 2003; Waksman et al., 1976). Fluorescent analogues of the natural nAChR agonists epibatidine and anabaseine have also recently been described and used for more selective nAChR fluorescent studies (Grandl et al., 2007; Talley et al., 2006).

Fluorophore-conjugated natural antagonists have also been utilized, with in many cases the highly potent peptidic snake toxin  $\alpha$ -bungarotoxin ( $\alpha$ -BgTx) conjugated to a wide range of different fluorophores including rhodamine, fluorescein isothiocyanate (FITC), Alexa dyes or biotin, for use in immunofluorescence studies with streptavidin-linked fluorophores (Anderson and Cohen, 1974; Baier et al., 2010; Bruneau et al., 2005; Qu et al., 1990; Wheeler et al., 1994). Other natural peptidic antagonists used in fluorescent studies include  $\alpha$ -cobratoxin and conotoxins (Hone et al., 2009; Johnson et al., 1990; Yang et al., 2011). However, there have been no reports to date of the conjugation of fluorophores to non-peptide (i.e. small-molecule) nAChR antagonists.

Pinnatoxin F (PnTX-F) is a member of the pinnatoxin family, produced by the dinoflagellate species *Vulcanodinium rugosum* (Nézan and Chomérat, 2011; Rhodes et al., 2011). As a member of the cyclic imine group of toxins, PnTX-F contains a 6, 7-linked cyclic imine moiety within its chemical structure (Fig 1). This moiety is thought to be the key structural requirement for the toxicity of this toxin group, which also includes gymnodimines, spirolides, pteriatoxins and prococontrolides (Molgó et al., 2007).

PnTX-F is highly toxic in rodent bioassays, causing death within minutes via respiratory depression (Munday et al., 2012; Selwood et al., 2010). Such activity is believed to be due to the pinnatoxins' ability to bind to and antagonize both muscle-type and neuronal nAChRs. In particular, PnTX-F has demonstrated low nanomolar inhibition of neuromuscular transmission *in vitro* (Araoz et al., 2011; Hellyer et al., 2013; Hess et al., 2013).

The aim of the current study was to conjugate a red fluorescent dye (VivoTag<sup>®</sup> 645) to PnTX-F, to enable visualization of PnTX-F binding at the mammalian NMJ. The biological and physical properties of the VivoTag<sup>®</sup> coupled pinnatoxin were examined using *in vitro* and *in vivo* toxicity studies and *in vitro* fluorescent co-localisation studies in muscle sections from *thy1-YFP-H* transgenic mice, whose motor nerves express yellow fluorescent protein (YFP).

## 2. Materials and methods

### 2.1. Synthesis of aminated pinnatoxin F derivatives

Pure PnTX-F was isolated from cultured *Vulcanodinium rugosum* cells, following previously described procedures (Selwood et al., 2010). All reactions were monitored by LC–MS using a Waters Acquity uPLC (Waters, Milford, MA) coupled to a Waters–Micromass Quattro Premier triple quadrupole mass spectrometer (Manchester, U.K.).

1.4 mmol of 2,2'-(ethylenedioxy)bis(ethylamine) (Sigma–Aldrich, St Louis, MO) was added to 0.52  $\mu$ moles of dry PnTX-F, and the mixture was then heated to 50° C. The reaction was complete after 3 h. The product PnTX-F–Sp1 was separated from the excess 2,2'-(ethylenedioxy)bis(ethylamine) over a 200 mg Strata-X SPE cartridge (Phenomenex, Torrance, CA) using a water/methanol stepwise gradient. Fractions containing PnTX-F–Sp1 were combined and dried under a stream of nitrogen. A smaller quantity of PnTX-F–Sp2 was prepared following this protocol using the diaminopolyether 4,7,10-trioxa-1,13-tridecanedimine.

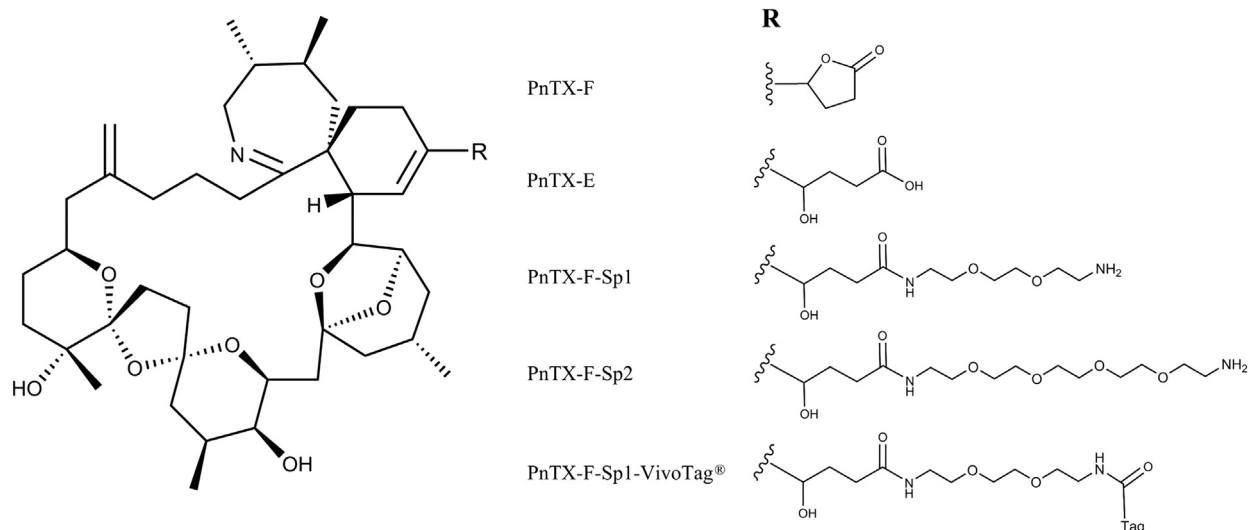


Fig. 1. Chemical structures of pinnatoxin F and derivatives.

## 2.2. Coupling of VivoTag<sup>®</sup> 645 to aminated pinnatoxin F

0.65  $\mu$ moles of VivoTag<sup>®</sup> 645 (PerkinElmer, Waltham, MA) in 90  $\mu$ L DMSO along with 20  $\mu$ L 5% DMAP in DMSO was added to dry PnTx-F–Sp1 at 20° C. The dry weight of PnTx-F Sp1 was unknown due to there being too little to accurately weigh. However, the reaction with the fluorophore appeared to be quantitative, as no other pinnatoxin analogues were detected after the reaction. The reaction was complete after 45 min. The tagged product PnTx-F–Sp1–VivoTag<sup>®</sup> was separated from the unreacted VivoTag<sup>®</sup> 645 over a 1 g Strata-X SPE cartridge (Phenomenex, Torrance, CA) with a water/methanol stepwise gradient containing 0.1% formic acid. Fractions containing PnTx-F–Sp1–VivoTag<sup>®</sup> were combined and dried under a stream of nitrogen. It was determined that there were 0.29  $\mu$ moles of PnTx-F–Sp1–VivoTag<sup>®</sup> by measuring the UV absorbance at 645 nm and using the molar extinction coefficient of VivoTag<sup>®</sup> 645.

## 2.3. In vitro toxicity

All procedures were approved by the University of Otago Animal Ethics Committee and conducted in accordance with the New Zealand Animal Welfare Act. Male Sprague–Dawley rats (6–8 weeks old) were obtained from the University of Otago Hercus-Taieri animal colony and housed for at least one week in the departmental holding facility on a 12 hr light–dark cycle, with free access to food and water. Rats were anaesthetised with CO<sub>2</sub> and sacrificed by rapid decapitation. Hemidiaphragms with attached phrenic nerves were dissected into Krebs-Henseleit buffer, consisting of (in mM) 120 NaCl, 2.5 CaCl<sub>2</sub>, 4.7 KCl, 2.1 MgSO<sub>4</sub>, 1.2 KH<sub>2</sub>PO<sub>4</sub>, 25 NaHCO<sub>3</sub> and 11 glucose, which had been saturated with 95% O<sub>2</sub>/5% CO<sub>2</sub> prior to use. Hemidiaphragms were then cleaned of extraneous tissue and immediately transferred to a holding chamber containing Krebs-Henseleit buffer maintained at room temperature and saturated with 95% O<sub>2</sub>/5% CO<sub>2</sub>.

Isolated phrenic-hemidiaphragm preparations were mounted in organ baths (40 mL volume) and superfused with oxygenated Krebs-Henseleit buffer. Organ bath temperature was maintained at 34–37° C. Each preparation was attached to a force transducer in order to record muscle tension, with resting tension adjusted to 2 g. The phrenic nerve of each preparation was drawn through the loops of a bipolar electrode connected to a Grass SD9 stimulator (Grass Instruments, West Warwick, RI, USA). Preparations were then left for up to 1 h to equilibrate. Following equilibration, motor nerve-evoked muscle twitches were recorded in response to square wave pulses of 0.1 ms duration and supramaximal voltage (usually ~10 V) delivered at 0.2 Hz. All twitch response waveforms were acquired digitally at 10 kHz, amplified and displayed on an eMac computer using a PowerLab 2/25 analogue digital converter (AD Instruments, Sydney). Recordings were monitored and stored using Chart<sup>™</sup> analytical software (Version 6–7, AD Instruments, Sydney) for offline analysis.

After maintenance of stable baseline twitch responses, spacer-modified (PnTx-F–Sp1/PnTx-F–Sp2) or fluorescently

labelled pinnatoxin F (PnTx-F–Sp1–VivoTag<sup>®</sup>) were added directly to the organ bath at various concentrations. Twitch tension was then monitored for up to 2 h, or until abolition of the response was observed. This was followed by a washout period of up to 2 h, in which fresh buffer was applied every 20–30 min.

All twitch response data is presented as mean  $\pm$  SEM. Graphs were constructed using GraphPad Prism (version 5.02).

## 2.4. In vivo toxicity

A 50  $\mu$ g sample of PnTx-F–Sp1–VivoTag<sup>®</sup> was dissolved in 500  $\mu$ L of methanol, and 50  $\mu$ L aliquots of the resulting solution were transferred into glass vials. Solvent was removed from these aliquots under nitrogen, and the dried sub-samples were stored at 20° C.

The median lethal dose of PnTx-F–Sp1–VivoTag<sup>®</sup> was determined according to the principles of OECD Guideline 425, and LD<sub>50</sub> values and 95% confidence intervals were calculated using the Acute Oral Toxicity (Guideline 425) Statistical Program (AOT425statPgm, version 1.0). The test material was dissolved in 1% Tween<sup>®</sup> 60 in normal saline. Aliquots of this solution, made up to a total volume of 1 mL with Tween<sup>®</sup> 60-saline, were injected intraperitoneally into female Swiss mice of initial body weight 18–22 g. The mice were monitored intensively during the day of dosing. Survivors were examined and weighed daily for the following 13 d, after which they were sacrificed killed and necropsied. The weights of liver, kidneys, spleen, heart and lungs were recorded at necropsy. Tap water and food (Rat and Mouse Cubes, Speciality Feeds Ltd, Glen Forrest, Western Australia) were available at all times.

## 2.5. Fluorescent labelling

*Thy1* YFP-H mice were anaesthetised with pentobarbitone, and transcardially perfused with warm heparinised saline followed by warm, fresh 4% paraformaldehyde in 0.1 M phosphate buffer. Individual extensor digitorum longus (EDL) muscles were dissected out, cryoprotected by immersion overnight in 20% sucrose in PBS, then embedded in OCT embedding compound and snap-frozen in isopentane cooled by liquid nitrogen, and finally stored at –20° C. Muscle samples were then cut into 16  $\mu$ m-thick transverse sections using a Leica 1850 cryostat (Leica Biosystems, Wetzlar, Germany). Sections were transferred to Polysine<sup>®</sup> microscope slides and allowed to air-dry for two min, after which time they were stored in a dark slide-chamber containing 1X phosphate-buffered saline (PBS-1X) until staining. Slides were stained with 200 nM or 1  $\mu$ M PnTx-F–Sp1–VivoTag<sup>®</sup> for 1 h. In fluorescent binding-inhibition studies, slides were pre-incubated with either 1  $\mu$ M  $\alpha$ -BgTx or 1  $\mu$ M PnTx-F for up to 1.5 h, followed by treatment with PnTx-F–Sp1–VivoTag<sup>®</sup> for 1 h. Control slides were incubated with PBS for an equal amount of time, prior to labelling with PnTx-F–Sp1–VivoTag<sup>®</sup>. Treated muscles were washed with PBS, and mounted with ProLong<sup>®</sup> Gold AntiFade reagent under a coverslip for confocal microscopy imaging.

## 2.6. Confocal microscopy

Fluorescent signals in the muscle sections were imaged with the use of a Zeiss 710 confocal laser-scanning microscope (Carl Zeiss Microscopy, Jena, Germany). To evaluate the motor endplates, two spectral windows using Zeiss ZEN 2009 software were captured. One window included the emission profile of YFP (excited using a 488 nm argon (Ar) laser) and the other included the emission profile of the VivoTag<sup>®</sup> 645 attached to PnTx-F (excited using a 633 nm helium–neon laser (HeNe) laser). All imaging parameters (laser intensity, gain, averaging, pinhole size) were kept constant throughout imaging.

Quantification of the fluorescent intensity at stained endplates was carried out via a threshold method using Image J (NIH) software in order to determine relative fluorescence in the absence and presence of inhibitors of PnTX-F–Sp1–VivoTag<sup>®</sup> binding. Briefly, images were background-subtracted before a threshold was imposed in order to determine the mean gray intensity of pixels in set regions of interest. The latter were defined as endplate regions where there was co-localisation of the green (YFP) and red (VivoTag<sup>®</sup> 645) fluorescent signals. In sections pre-incubated with inhibitors, gain was increased to visualize the red signal and identify regions of interest, before being returned to baseline values for fluorescent measurements. Threshold values were kept consistent over all groups of sections. Mean gray value fluorescent intensities were compared using a one-way ANOVA with a Dunnett's post-hoc test. All data are presented as mean  $\pm$  SEM.

## 3. Results

### 3.1. In vitro toxicity

Both the polyether spacer-modified PnTx-F derivatives (PnTX-F–Sp1 and PnTX-F–Sp2) and the fluorescent conjugate (PnTX-F–Sp1–VivoTag<sup>®</sup>) were tested in a rat phrenic-nerve hemidiaphragm preparation for *in vitro* neuromuscular toxicity. As limited amounts of each

compound were available, toxicity was only assessed at 1 or 2 concentrations, and in a small number of preparations.

When tested at 50 nM, PnTX-F–Sp1 and PnTX-F–Sp2 caused a reduction in the nerve-evoked twitch response in hemidiaphragm preparations (Fig. 2A). After 30 min of exposure to PnTX-F–Sp1, the hemidiaphragm twitch response was reduced to  $24 \pm 23\%$  of baseline, while PnTX-F–Sp2 reduced the response to  $36 \pm 0.8\%$  of baseline. Both derivatives caused a greater than 90% inhibition of the twitch response after 60 min exposure. The neuromuscular-blocking actions of both derivatives were reversed by a 1 h washout period, with the twitch response returning to 75–90% of baseline after this treatment (Fig. 2B).

PnTX-F–Sp1 exhibited slightly higher toxicity and a more favourable washout profile than PnTX-F–Sp2 (i.e. slower washout and therefore more favourable for use in fluorescent binding studies which include multiple wash steps). Thus it was chosen for conjugation to the VivoTag<sup>®</sup> 645 fluorophore. The resultant PnTX-F–Sp1–VivoTag<sup>®</sup> was found to have further decreased toxicity relative to PnTX-F–Sp1 (Fig. 3). PnTX-F–Sp1–VivoTag<sup>®</sup> at 200 nM and 500 nM only reduced the hemidiaphragm twitch response to  $92 \pm 1.6\%$  and  $69 \pm 13\%$  of baseline, respectively. Even after 60 min of exposure to PnTX-F–Sp1–VivoTag<sup>®</sup>, hemidiaphragms still exhibited twitch responses 35–70% of baseline. In those preparations exposed to 500 nM that showed significant reductions in twitch response, washouts were undertaken, and twitch responses subsequently returned to 90% of baseline within 20 min (data not shown).

### 3.2. In vivo toxicity

The LD<sub>50</sub> of the fluorescent conjugate was 126  $\mu\text{g}/\text{kg}$ , with 95% confidence limits between 110 and 169  $\mu\text{g}/\text{kg}$  (Table 1). On a molar basis, this median lethal dose is 66.7 nmol/kg, with 95% confidence limits between 58.2 and 89.4 nmol/kg. These values represent a 4-fold loss in potency relative to native PnTx-F, which has a median lethal dose of 16–20 nmol/kg (Table 1).

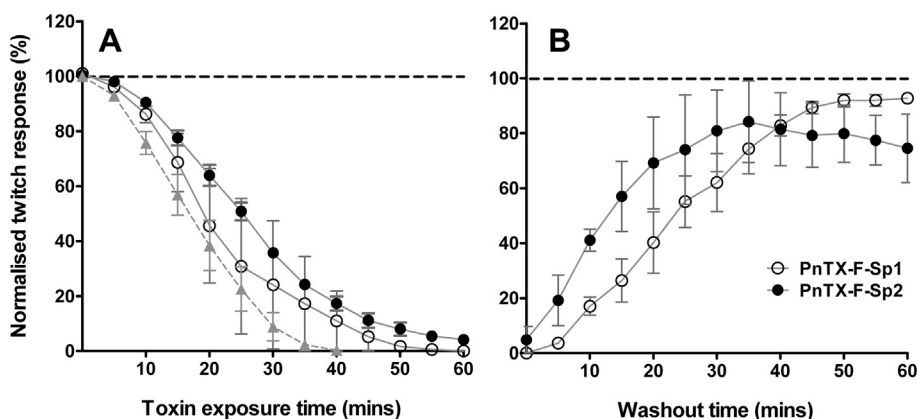


**Fig. 2.** Effect of polyether-spacer–PnTx-F derivatives (PnTX-F–Sp1 and PnTX-F–Sp2) on *in vitro* rat hemidiaphragm responses. (A) Dot plots showing time-course of PnTX-F–Sp1 and PnTX-F–Sp2 effects on phrenic nerve-evoked hemidiaphragm twitch responses. Toxin was added at time point zero. Dotted line represents the time course of native PnTx F (25 nM; from Hellyer et al., 2013). (B) Dot plot showing recovery of muscle twitch responses during PnTX-F–Sp1 and PnTX-F–Sp2 washout. Preparations were perfused with fresh buffer every 15–20 min for 1 h. All points represent the normalized twitch response, expressed as mean  $\pm$  SEM of 2 muscle preparations.

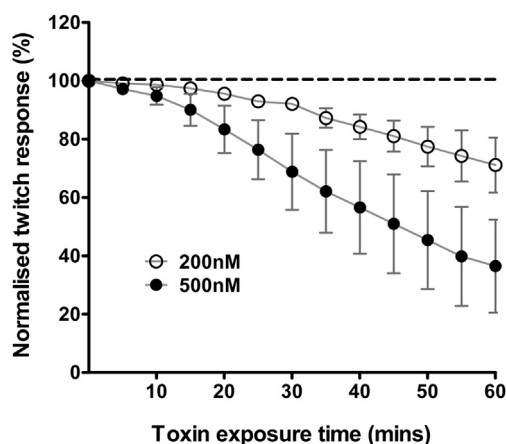


**Fig. 3.** Time-course and concentration-dependence of the neuromuscular-blocking activity of fluorescently labelled pinnatoxin F (PnTX-F-Sp1-VivoTag<sup>®</sup>) in rat phrenic nerve-evoked hemidiaphragm preparations. PnTX-F-Sp1-VivoTag<sup>®</sup> was added at time point zero. All points represent the normalized twitch response, expressed as mean % of baseline  $\pm$  SEM of 3 muscle preparations.

Symptoms of intoxication from PnTX-F-Sp1-VivoTag<sup>®</sup> were similar to those recorded with other pinnatoxin derivatives. At lethal doses, mice were initially active, but activity subsequently declined, and the animals became immobile, with marked abdominal breathing. At this time, respiration rates declined, and death from respiratory failure occurred at 13–25 min post-injection. At sublethal (but toxic) doses, mice became lethargic, displaying abdominal breathing soon after administration of test substance, but recovered fully by ~1.5 h post-dosing. No deaths were recorded at doses of 100, 79 or 63  $\mu$ g/kg, although signs of toxicity were observed. No adverse effects were seen at a dose of 50  $\mu$ g/kg.

### 3.3. Fluorescence microscopy

Expression of YFP in *thy1-YFP-H* transgenic mice enables direct visualization of motor nerves in muscle sections using fluorescence and confocal microscopy. Such presynaptic labelling at the NMJ allows utilization of labelled neuromuscular-blocking agents to reveal pre- or post-synaptic binding at the synapse. Fluorescent labelling of muscle sections was effected by PnTX-F-Sp1-VivoTag<sup>®</sup>, with the red signals arising from this conjugate co-localised with green YFP signals in EDL muscle sections (Fig. 4). Labelling was concentration-dependent, with higher fluorescence intensity achieved when muscle sections were stained with 1  $\mu$ M ( $38.7 \pm 3.0$  mean gray units,  $n = 72$

**Table 1**

Median lethal doses of PnTX-E, -F and PnTX-F-Sp1-VivoTag<sup>®</sup> by intraperitoneal injection.

Compound	LD <sub>50</sub> (nmol/kg) <sup>a</sup>	Reference
PnTX-F-Sp1-VivoTag <sup>®</sup>	66.7 (58.2–89.4)	This work
PnTx F	16.6 (12.4–19.1)	Munday et al. (2012)
	20.9 (15.7–30.0)	Selwood et al. (2010)
PnTx E	72.7 (50.6–96.0)	Munday et al. (2012)
	57.4 (40.8–74.0)	Selwood et al. (2010)

<sup>a</sup> Figures in brackets indicate 95% confidence intervals.

endplates) than with 200 nM PnTX-F-Sp1-VivoTag<sup>®</sup> ( $26.8 \pm 1.3$  mean gray units,  $n = 95$  endplates).

Most red fluorescent signals were closely associated with the green YFP signals, and vice versa. However, some individual red and green signals were observed, with these most likely due to unlabelled motor nerves present in the section, or the separation of pre- and post-synaptic elements during the sectioning process. At endplates in which both signals were present, PnTX-F-Sp1-VivoTag<sup>®</sup> labelled areas adjacent to the YFP-containing nerve terminals, with little overlap of the signals observed. Almost no diffuse fluorescent signal was observed in other areas of the muscle sections, indicating specific binding of PnTX-F-Sp1-VivoTag<sup>®</sup> at the endplates. Taken together, these observations suggest that PnTX-F-Sp1-VivoTag<sup>®</sup> is binding at the post-synaptic membrane of the NMJ.

Given that pinnatoxins have been shown to bind to muscle-type nAChRs, it was assumed that the fluorescent labelling represented labelling of these receptors. To test this, fluorescent binding studies were carried out in the presence of unlabelled  $\alpha$ -BgTx, a known high-affinity antagonist for muscle-type nAChRs (Fig. 5). Pre-incubation of muscle sections with 1  $\mu$ M  $\alpha$ -BgTx reduced the intensity of the red fluorescent PnTX-F-Sp1-VivoTag<sup>®</sup> signal to  $12.7 \pm 3.9\%$  ( $n = 48$  endplates) of levels seen with no inhibitor present, indicating that  $\alpha$ -BgTx and PnTX-F-Sp1-VivoTag<sup>®</sup> are binding at the same site i.e. muscle-type nAChRs. Pre-incubation of the muscle sections with 1  $\mu$ M PnTx-F also reduced the intensity of fluorescence to  $25.8 \pm 7.1\%$  of baseline levels ( $n = 27$  endplates). This confirms that the conjugation of the fluorescent label does not change the receptor target of PnTX-F, as PnTX-F-Sp1-VivoTag<sup>®</sup> and PnTx-F compete for the same binding site.

## 4. Discussion

Fluorescent labels are important tools in the study of receptors and their interactions with various ligands. Here we describe the synthesis of the first example of a fluorophore-conjugated small-molecule nAChR antagonist, PnTX-F-Sp1-VivoTag<sup>®</sup>, for use in fluorescent-labelling studies at the mammalian NMJ. PnTX-F-Sp1-VivoTag<sup>®</sup> efficaciously labelled endplates of motor nerves of mouse muscle sections, and retained neuromuscular blocking abilities *in vitro*, as well as displaying *in vivo* toxicity (albeit with reduced potency compared to PnTX-F).

The initial step in the synthesis of PnTX-F-Sp1-VivoTag<sup>®</sup> was the addition of an amine-capped polyether spacer to the cyclohexene ring of PnTX-F. The incorporation of this spacer unit was deemed necessary as VivoTag<sup>®</sup>645, like many fluorophores, is a large molecule (i.e. 1393 g/mol, c.f. 766 g/mol for PnTX-F), so it was important to physically separate it from the pharmacologically active portion of PnTX-F, to minimize the chance of steric occlusion of key recognition/binding moieties. Analogous spacer-based approaches to small-molecule fluorescent nAChR agonists have been described (Grandl et al., 2007; Krieger et al., 2008; Meyers et al., 1983; Waksman et al., 1976), where the potency of the fluorophore-agonist conjugate generally increases with the length of the spacer in the conjugate.

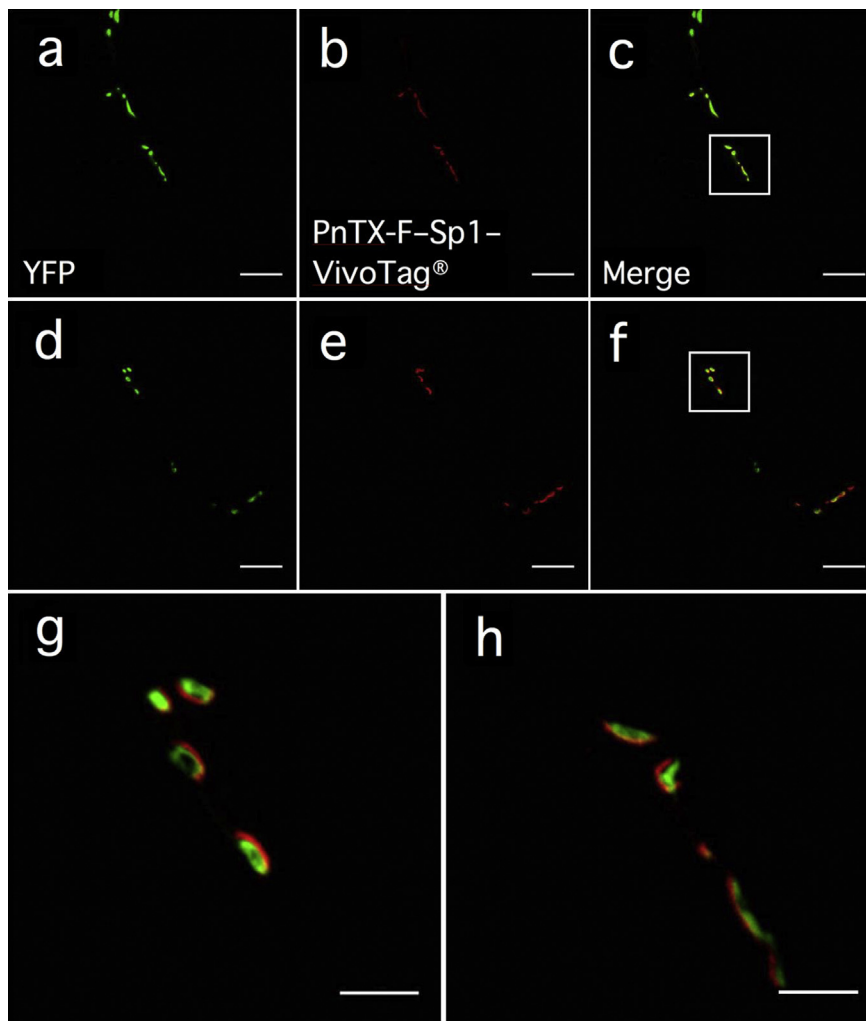


**Fig. 4.** PnTX-F-Sp1-VivoTag<sup>®</sup> labelling of endplates in YFP-motor nerve-containing EDL muscle from *thy-1* YFP-H mice. (a–f) Localisation of the YFP containing motor nerve endings (green, a & d) with the PnTX-F-Sp1-VivoTag<sup>®</sup> fluorescent signal (red, b & e), with composite images showing relative staining (c & f). The white boxes in the composite images c and f are expanded in images g and h, respectively. Red PnTX-F-Sp1-VivoTag<sup>®</sup> signals are located in areas adjacent to the YFP motor nerves, indicating staining of the post-synaptic density at the neuromuscular junction. Images a–f were taken with a laser scanning microscope at 63x magnification, with images g and h at 300x magnification. Scale bars represent 20  $\mu$ m (a–f) and 5  $\mu$ m (g and h).

Interestingly, dansyl-acetylcholine conjugates have been described which are nAChR antagonists when the spacer comprised a 1- or 2-carbon linker, but nAChR agonists when the spacer comprised 3–6 carbons, with potency proportional to spacer chain-length (Waksman et al., 1976). The antagonist activity may be due to the dansyl moiety being close enough (in these short-spacer conjugates) to the main acetylcholine molecule to prevent the closure of loop-C of the nAChR (Brams et al., 2011).

For fluorescent antagonist studies using large peptides such as  $\alpha$ -BgTx, the spacer is less important, given the size of the ligand recognition domain compared to the whole molecule. However, for small-molecule antagonists such as PnTX-F, the addition of a spacer is assumed to be more critical, as it allows the fluorescent conjugate to retain as much of its nAChR-binding affinity as possible, although this hypothesis was not directly tested in this study.

The spacer-modified versions of PnTX-F, PnTX-F-Sp1 and PnTX-F-Sp2, proved to have reduced *in vitro* neuromuscular-blocking potency. At 50 nM, PnTX-F-Sp1 and PnTX-F-Sp2 reduced twitch responses to 24–36% of baseline after 30 min, with almost complete recovery after washout. In contrast, identical preparations dosed with 25 nM PnTX-F exhibited greater than 90% reduction of twitch responses at 30 min and only partial (less than 40%) recovery after two hours of washout (Hellyer et al., 2013). The antagonist potencies of PnTX-F-Sp1 and PnTX-F-Sp2 are in fact comparable to PnTX-E (the open-ring analogue of PnTx-F), which reduces hemidiaphragm twitch responses to around 60% of baseline after 30 min exposure at 50 nM, and which exhibits ready reversal following washout, even at high concentrations (Hellyer et al., 2013).

The reduction in activity of PnTX-F-Sp1 and PnTX-F-Sp2 may be due to the replacement of the lactone side

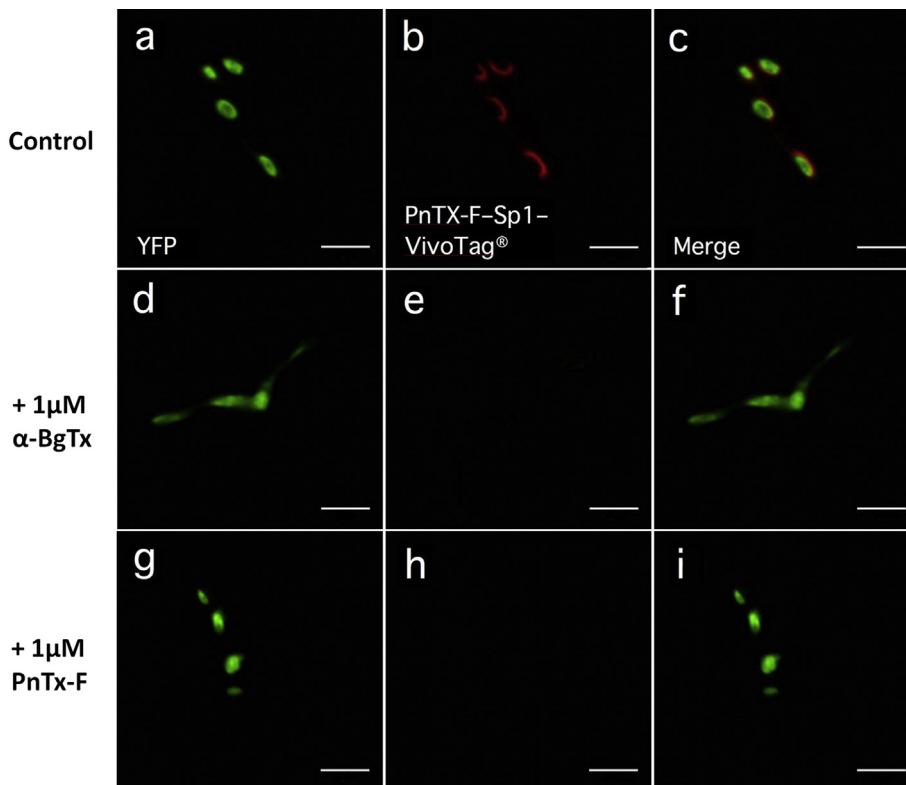


**Fig. 5.** Effect of alpha-bungarotoxin ( $\alpha$ -BgTx) and pinnatoxin F (PnTx-F) on PnTx-F–Sp1–VivoTag<sup>®</sup>-labelling of endplates in *thy-1* YFP mouse muscle sections. (a–c) Control sections show intense staining of endplates, with red PnTx-F–Sp1–VivoTag<sup>®</sup> signals adjacent to those of the YFP-containing nerve terminals. (d–f) Pre-incubation of muscle sections for 60 min with 1  $\mu$ M  $\alpha$ -BgTx almost abolished PnTx-F–Sp1–VivoTag<sup>®</sup> labelling. (g–i) Pre-incubation of muscle sections with 1  $\mu$ M PnTx-F reduced the red fluorescent PnTx-F–Sp1–VivoTag<sup>®</sup> signal. All images were taken with a laser-scanning microscope at 300x magnification. Scale bars represent 5  $\mu$ m.

chain of PnTx-F with the spacer. This is supported by the observation that pinnatoxin E (PnTx-E), which has the corresponding acyclic  $\gamma$ -hydroxybutanoic acid group rather than a lactone, is also less potent than PnTx-F and is more easily reversed by washout (Hellyer et al., 2013). This reduction in potency of both PnTx-E and the spacer-modified derivatives suggests that the lactone ring, a feature that is also found in the structurally related spirolides (Bourne et al., 2010), may be important for high affinity pinnatoxin binding.

Conjugation of the VivoTag<sup>®</sup> fluorophore to PnTx-F–Sp1 and PnTx-F–Sp2 resulted in labelled conjugates with further reduced neuromuscular-blocking activity relative to the natural product. Concentrations of PnTx-F–Sp1–VivoTag<sup>®</sup> as high as 500 nM produced only a ~30% reduction in twitch response over a 30 min test period, with these effects easily reversed after a short washout period.

Reduced potency has been reported in other fluorophore–antagonist conjugate studies. For example, conjugation of fluorescein isothiocyanate (FITC) or tetramethylrhodamine-5-(and-6)-isothiocyanate [(5(6)-TRITC)] to the peptidic antagonist  $\alpha$ -BgTx resulted in a 2–100 fold reduction in potency of the fluorescent conjugate, *in vitro* and *in vivo*, relative to the native toxin (Anderson and Cohen, 1974). Similarly, Alexa 488-conjugated  $\alpha$ -BgTx displayed a 50-fold reduction in

potency in radioligand binding studies using a cell line expressing  $\alpha 7$  nAChRs (Shelukhina et al., 2009). Also, fluorescent conjugates of the naturally occurring nAChR agonist epibatidine displayed a decrease in binding affinity of 1–3 orders of magnitude, in addition to a reduced ability to activate a wide range of nAChRs (Grandl et al., 2007).

Although sufficient data for full concentration–response curves could not be obtained, it is clear that the *in vitro* potency of PnTx-F–Sp1–VivoTag<sup>®</sup> is considerably less than that of PnTx-F, which blocks the twitch response in an *in vitro* hemidiaphragm preparation with an IC<sub>50</sub> of 11 nM (Hellyer et al., 2013). Surprisingly however, the *in vivo* potency of PnTx-F–Sp1–VivoTag<sup>®</sup> is only approximately four times less than that of PnTx-F, and PnTx-F–Sp1–VivoTag<sup>®</sup> has a similar LD<sub>50</sub> to PnTx-E (Munday et al., 2012; Selwood et al., 2010).

This *in vivo* potency profile for PnTx-F–Sp1–VivoTag<sup>®</sup> is similar to that seen *in vitro* for PnTx-F–Sp1. It is possible that endogenous *in vivo* esterase activity is responsible for cleaving the ester-like bond between the fluorophore and the spacer of PnTx-F–Sp1–VivoTag<sup>®</sup>, and suggests that the *in vivo* toxicity of PnTx-F–Sp1–VivoTag<sup>®</sup> is in fact due to the presence of the PnTx-F–Sp1, rather than PnTx-F–Sp1–VivoTag<sup>®</sup> itself.

Despite the fact that spacer-mediated attachment of VivoTag<sup>®</sup>645 gave fluorophore-labelled analogues of PnTx-

F with decreased neuromuscular-blocking activity, the PnTX-F–Sp1–VivoTag<sup>®</sup> was nevertheless able to specifically label endplates in *thy-1* mouse muscle sections in a concentration-dependent manner. However, as suggested by the *in vitro* toxicity data, staining of muscle sections with 200 nM PnTX-F–Sp1–VivoTag<sup>®</sup> did not saturate binding sites, although a concentration of 1  $\mu$ M generated ~1.5 times greater intensity of staining.

Only short (10 min) washout periods were used after staining of tissue with PnTX-F–Sp1–VivoTag<sup>®</sup>, due to the observed rapid reversibility of binding in *in vitro* toxicity studies. This differs from most protocols, which utilise longer and more rigorous washout procedures in attempt to reduce non-specific binding. However, despite the short washout, PnTX-F–Sp1–VivoTag<sup>®</sup> showed very little non-specific binding. A majority of the red signal from PnTX-F–Sp1–VivoTag<sup>®</sup> was closely associated with the YFP-containing motor nerves, and the intensity of staining was reduced by ~90% in the presence of unlabelled  $\alpha$ -BgTx, indicating specific binding to nAChRs at the endplates. Red signals that were not associated with green signals were still intensely localised, rather than diffuse, and probably indicate endplates that were either separated from the motor nerve due to the sectioning procedure, or those whose motor nerve did not contain YFP. With respect to the latter possibility, it is known that the *thy-1* YFP-H strain of mice used in the current study does not express the YFP transgene in every motor axon, meaning that there will be endplates present that are not associated with a YFP-containing motor nerve (Feng et al., 2000).

Endplate labelling by PnTX-F–Sp1–VivoTag<sup>®</sup> was also inhibited by prior incubation of muscle sections with native PnTX-F, indicating that the addition of the fluorophore was not changing the binding target of the pinnatoxins. Taken together with the observations that labelling could be inhibited by  $\alpha$ -BgTx, these data suggest that PnTX-F–Sp1–VivoTag<sup>®</sup> is a specific stain for nAChRs at the motor endplate, and that this is the target of the pinnatoxins in their natural state. This is supportive of recent data showing that PnTX-A binds to and antagonises nAChRs of the both the muscle and neuronal subtypes, and that PnTX-E, -F and -G are potent blockers of transmission at the NMJ, with their effects indicative of nAChR antagonist activity (Araoz et al., 2011; Hellyer et al., 2013).

The results obtained from the current study provide further evidence of the muscle-type nicotinic receptor binding activity of the pinnatoxins. To our knowledge, this study represents the first example of a small-molecule nAChR antagonist being conjugated with a fluorophore, to allow direct visualisation of nAChR binding. Although the reduced potency and less stable binding characteristics of PnTX-F–Sp1–VivoTag<sup>®</sup> may limit its use, this work nevertheless constitutes proof of principle and is an important step forward in the creation of more potent and specific small-molecule fluorescent antagonists of nAChRs.

### Ethical statement

All procedures were approved by the University of Otago Animal Ethics Committee, in accordance with the

New Zealand Animal Welfare Act, and in accordance with guidelines for the ethical and humane use of animals in research, established under the U.K. Animals (Scientific Procedures) Act 1986 (Chapter 14, Schedule 1, Table A).

### Acknowledgements

This study received funding from the European Union Seventh Framework Programme (FP7/2007–2013) under grant agreement n<sup>o</sup> 311820 (ECsafeSEAFOOD). The authors thank the Otago Centre for Confocal Microscopy (University of Otago, Dunedin, New Zealand) for use of the Zeiss microscope and technical support.

### Conflict of interest

The authors declare that there are no conflicts of interest.

### Transparency document

Transparency document related to this article can be found online at <http://dx.doi.org/10.1016/j.toxicol.2014.05.013>.

### References

- Anderson, M., Cohen, M., 1974. Fluorescent staining of acetylcholine receptors in vertebrate skeletal muscle. *J. Physiol.* 237, 385–400.
- Araoz, R., Servent, D., Molgó, J., Iorga, B.L., Fruchart-Gaillard, C., Benoit, E., Gu, Z., Stivala, C., Zakarian, A., 2011. Total synthesis of pinnatoxins A and G and a revision of the mode of action of pinnatoxin A. *J. Am. Chem. Soc.* 133, 10499–10511.
- Auerbach, A., 2003. Life at the top: the transition state of AChR gating. *Sci. Signal.* 2003, re11.
- Baier, C.J., Gallegos, C.E., Levi, V., Barrantes, F.J., 2010. Cholesterol modulation of nicotinic acetylcholine receptor surface mobility. *Eur. Biophys. J.* 39, 213–227.
- Barrantes, F., Sakmann, B., Bonner, R., Eibl, H., Jovin, T., 1975. 1-Pyrenebutyrylcholine: a fluorescent probe for the cholinergic system. *Proc. Natl. Acad. Sci.* 72, 3097–3101.
- Bourne, Y., Radi, Z., Aráoz, R., Talley, T., Benoit, E., Servent, D., Taylor, P., Molgó, J., Marchot, P., 2010. Structural determinants in phycotoxins and AChBP conferring high affinity binding and nicotinic AChR antagonism. *Proc. Natl. Acad. Sci.* 107, 6076–6082.
- Brams, M., Pandya, A., Kuzmin, D., van Elk, R., Krijnen, L., Yakel, J.L., Tsetlin, V., Smit, A.B., Ulens, C., 2011. A structural and mutagenic blueprint for molecular recognition of strychnine and d-tubocurarine by different cys-loop receptors. *PLoS Biol.* 9, e1001034.
- Bruneau, E., Sutter, D., Hume, R.I., Akaaboune, M., 2005. Identification of nicotinic acetylcholine receptor recycling and its role in maintaining receptor density at the neuromuscular junction *in vivo*. *J. Neurosci.* 25, 9949–9959.
- Cohen, J.B., Changeux, J.P., 1973. Interaction of a fluorescent ligand with membrane-bound cholinergic receptor from *Torpedo marmorata*. *Biochemistry* 12, 4855–4864.
- Edelstein, S.J., Schaad, O., Changeux, J.-P., 1997. Single binding versus single channel recordings: a new approach to study ionotropic receptors. *Biochemistry* 36, 13755–13760.
- Feng, G., Mellor, R.H., Bernstein, M., Keller-Peck, C., Nguyen, Q.T., Wallace, M., Nerbonne, J.M., Lichtman, J.W., Sanes, J.R., 2000. Imaging neuronal subsets in transgenic mice expressing multiple spectral variants of GFP. *Neuron* 28, 41–51.
- Grandl, J., Sakr, E., Kotzyba-Hibert, F., Krieger, F., Bertrand, S., Bertrand, D., Vogel, H., Goeldner, M., Hovius, R., 2007. Fluorescent epibatidine agonists for neuronal and muscle-type nicotinic acetylcholine receptors. *Angew. Chem.* 119, 3575–3578.
- Hellyer, S.D., Selwood, A.I., Rhodes, L., Kerr, D.S., 2013. Neuromuscular blocking activity of pinnatoxins E, F and G. *Toxicol* 76, 214–220.

- Hess, P., Abadie, E., Hervé, F., Berteaux, T., Séchet, V., Araújo, R., Molgó, J., Zakarian, A., Sibat, M., Rundberget, T., 2013. Pinnatoxin G is responsible for atypical toxicity in mussels *Mytilus galloprovincialis* and clams *Venerupis decussata* from Ingril, a French Mediterranean lagoon. *Toxicon* 75, 16–20.
- Hone, A.J., Whiteaker, P., Christensen, S., Xiao, Y., Meyer, E.L., McIntosh, J.M., 2009. A novel fluorescent  $\alpha$ -conotoxin for the study of  $\alpha 7$  nicotinic acetylcholine receptors. *J. Neurochem.* 111, 80–89.
- Johnson, D., Cushman, R., Malekzadeh, R., 1990. Orientation of cobra alpha-toxin on the nicotinic acetylcholine receptor. Fluorescence studies. *J. Biol. Chem.* 265, 7360–7368.
- Jürss, R., Prinz, H., Maelicke, A., 1979. NBD-5-acylcholine: fluorescent analog of acetylcholine and agonist at the neuromuscular junction. *Proc. Natl. Acad. Sci.* 76, 1064–1068.
- Krieger, F., Mourot, A., Araoz, R., Kotzyba-Hibert, F., Molgó, J., Bamberg, E., Goeldner, M., 2008. Fluorescent agonists for the Torpedo nicotinic acetylcholine receptor. *ChemBioChem* 9, 1146–1153.
- Meyers, H., Jürss, R., Brenner, H., Fels, G., Prinz, H., Watzke, H., Maelicke, A., 1983. Synthesis and properties of NBD-n-acylcholines, fluorescent analogs of acetylcholine. *Eur. J. Biochem./FEBS* 137, 399.
- Molgó, J., Girard, E., Benoit, E., 2007. 18 cyclic imines: an insight into this emerging group of bioactive marine toxins. In: Botana, L.M. (Ed.), *Phycotoxins: Chemistry and Biochemistry*. Wiley-Blackwell, pp. 319–335.
- Munday, R., Selwood, A.I., Rhodes, L., 2012. Acute toxicity of pinnatoxins E, F and G to mice. *Toxicon* 60, 995–999.
- Nézan, E., Chomérat, N., 2011. *Vulcanodinium rugosum* gen. et sp. nov. (Dinophyceae), un nouveau dinoflagellé marin de la côte méditerranéenne française. *Cryptogam. Algol.* 32, 3–18.
- Qu, Z., Moritz, E., Haganir, R.L., 1990. Regulation of tyrosine phosphorylation of the nicotinic acetylcholine receptor at the rat neuromuscular junction. *Neuron* 4, 367–378.
- Rhodes, L., Smith, K., Selwood, A., McNabb, P., Munday, R., Suda, S., Molenaar, S., Hallegraef, G., 2011. Dinoflagellate *Vulcanodinium rugosum* identified as the causative organism of pinnatoxins in Australia, New Zealand and Japan. *Phycologia* 50, 624–628.
- Selwood, A., Miles, C., Wilkins, A., van Ginkel, R., Munday, R., Rise, F., McNabb, P., 2010. Isolation, structural determination and acute toxicity of pinnatoxins E, F and G. *J. Agric. Food Chem.* 58, 6532–6542.
- Shelukhina, I.V., Kryukova, E.V., Lips, K.S., Tsetlin, V.I., Kummer, W., 2009. Presence of  $\alpha 7$  nicotinic acetylcholine receptors on dorsal root ganglion neurons proved using knockout mice and selective  $\alpha$ -neurotoxins in histochemistry. *J. Neurochem.* 109, 1087–1095.
- Song, X.-Z., Andreeva, I.E., Pedersen, S.E., 2003. Site-selective agonist binding to the nicotinic acetylcholine receptor from *Torpedo californica*. *Biochemistry* 42, 4197–4207.
- Talley, T.T., Yalda, S., Ho, K.-Y., Tor, Y., Soti, F.S., Kem, W.R., Taylor, P., 2006. Spectroscopic analysis of benzylidene anabaseine complexes with acetylcholine binding proteins as models for ligand-nicotinic receptor interactions. *Biochemistry* 45, 8894–8902.
- Waksman, G., Fournié-Zaluski, M.-C., Roques, B., Heidmann, T., Grünhagen, H.-H., Changeux, J.-P., 1976. Synthesis of fluorescent acylcholines with agonistic properties: pharmacological activity on *Electrophorus* electroplaque and interaction *in vitro* with *Torpedo* receptor-rich membrane fragments. *FEBS Lett.* 67, 335–342.
- Wheeler, S.V., Jane, S.D., Cross, K.M., Chad, J.E., Foreman, R.C., 1994. Membrane clustering and bungarotoxin binding by the nicotinic acetylcholine receptor: role of the  $\beta$  subunit. *J. Neurochem.* 63, 1891–1899.
- Yang, K., Buhlman, L., Khan, G.M., Nichols, R.A., Jin, G., McIntosh, J.M., Whiteaker, P., Lukas, R.J., Wu, J., 2011. Functional nicotinic acetylcholine receptors containing  $\alpha 6$  subunits are on GABAergic neuronal boutons adherent to ventral tegmental area dopamine neurons. *J. Neurosci.* 31, 2537–2548.